

TOWARD AUTOMATING PATIENT-SPECIFIC STRESS ANALYSIS FROM MEDICAL IMAGING



Omar Hafez
UC Davis

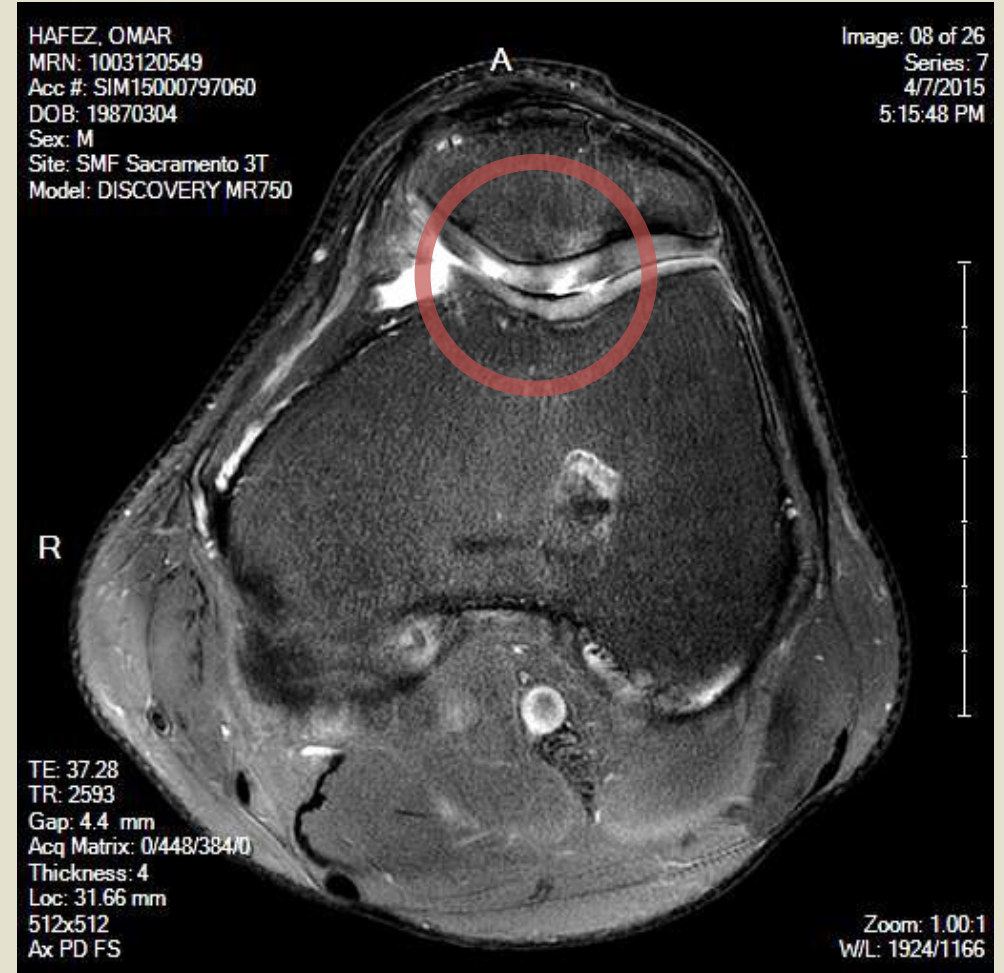
DOE CSGF Annual Program Review
28 July 2015 • Arlington, VA



A SHORT STORY



2009



2015

IN A NUTSHELL

Medical Imaging

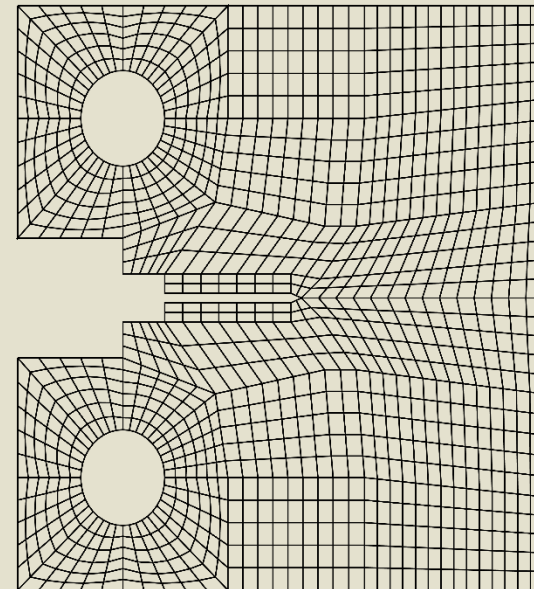
- X-ray, MRI, CT, ultrasound
- Used for diagnostics: identification of tumors, kidney stones, osteoarthritis



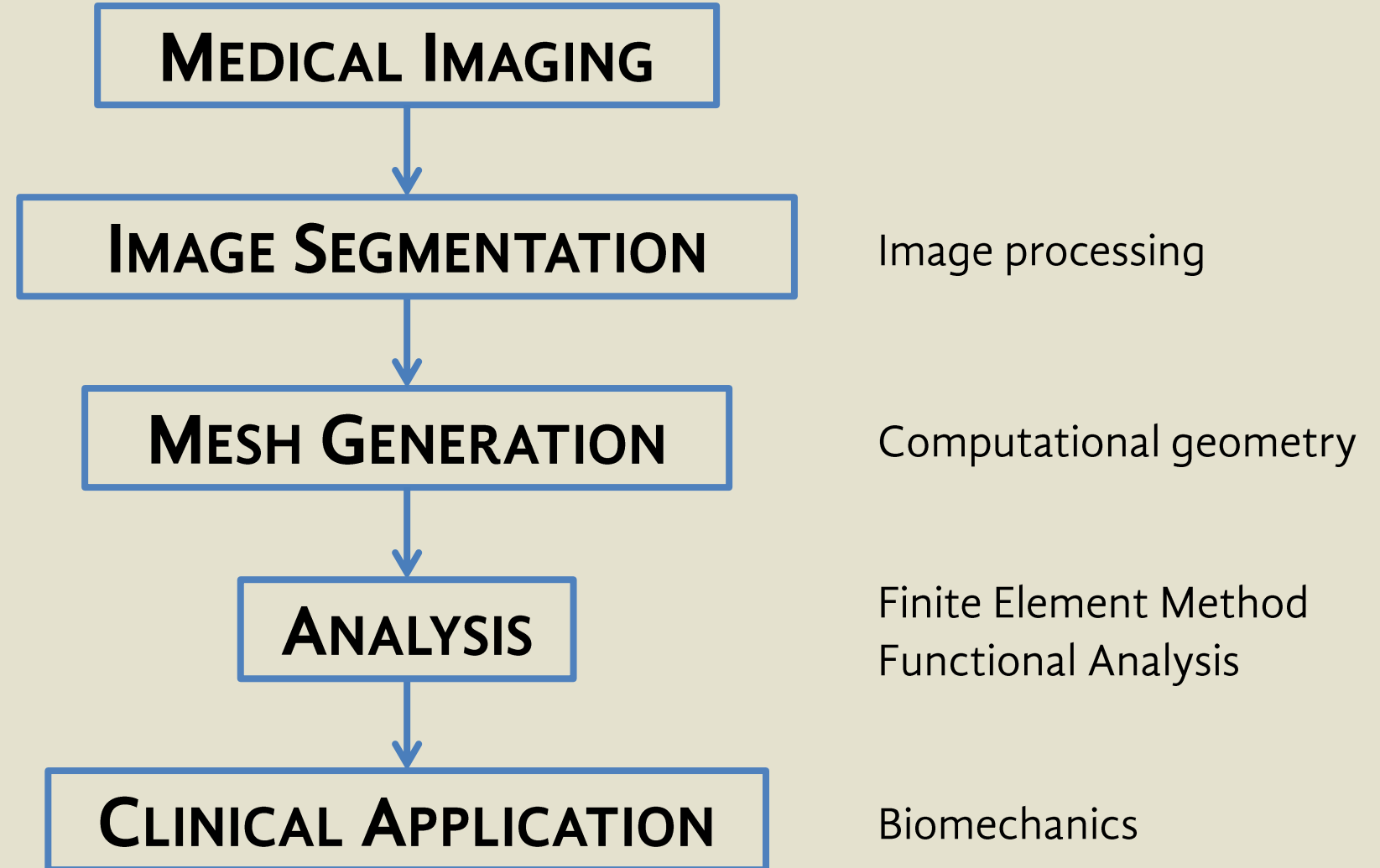
info.blockimaging.com/bid/98700/GE-MRI-Scanner-Cost-Price-Info

Physics-Based Simulation

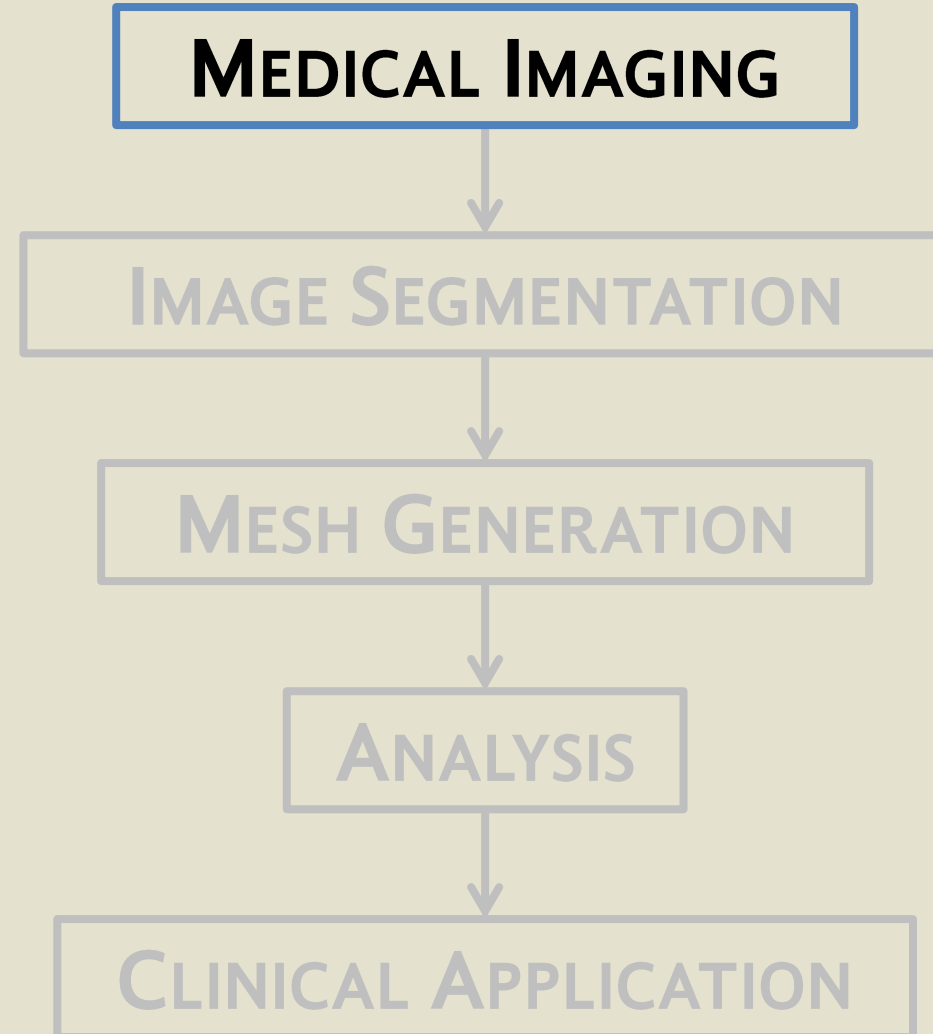
- FEM, meshless methods, finite volumes, finite differences
- Ability to provide engineering guidance to biomechanics problems



THE PIPELINE



THE PIPELINE



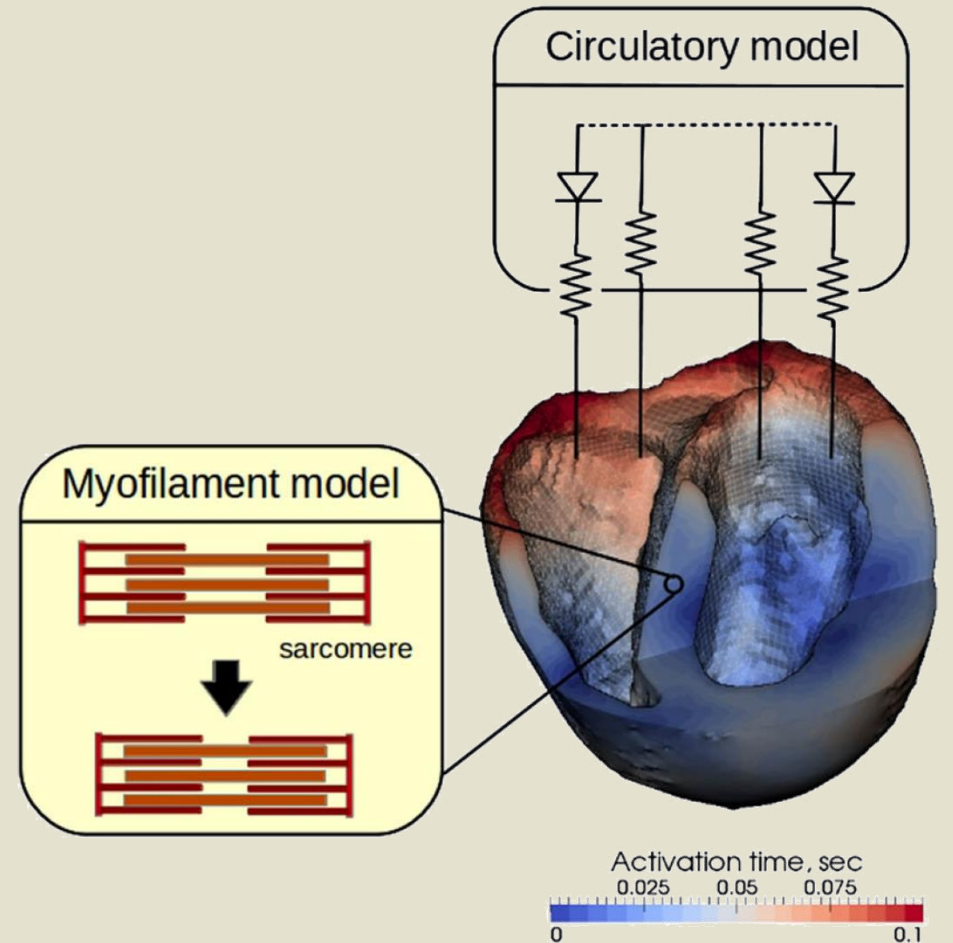
MAGNETIC RESONANCE IMAGING (MRI)

- Roughly measures the weighted proton density of each point in the field
- Set of 2D slices represent 3D data set
- Image resolution: $\sim 0.5 \times 0.5 \times 3$ mm
- MRI essentially provides 3D point intensity data



CARDIOID

- Joint venture of LLNL and IBM
- Sequoia: 20 PFLOPS, 98k nodes, 1.6m processors
- Electrophysiology + mechanics of human heart → mechanisms of sudden cardiac arrest from arrhythmia
- Highly efficient and scalable code → unprecedented exploration



MECHANICS

- Passive cardiac tissue modeled as a hyperelastic, incompressible material with orthotropic properties
- mixed pressure-displacement finite elements are used to enforce incompressibility
- Active stress is generated by a model with force dependence on length and velocity of muscle shortening

$$\frac{\partial}{\partial X_M} (T_{MN}(\mathbf{x}, p) F_{iN}(\mathbf{x})) + \rho g_i = 0$$

$$J = 1$$

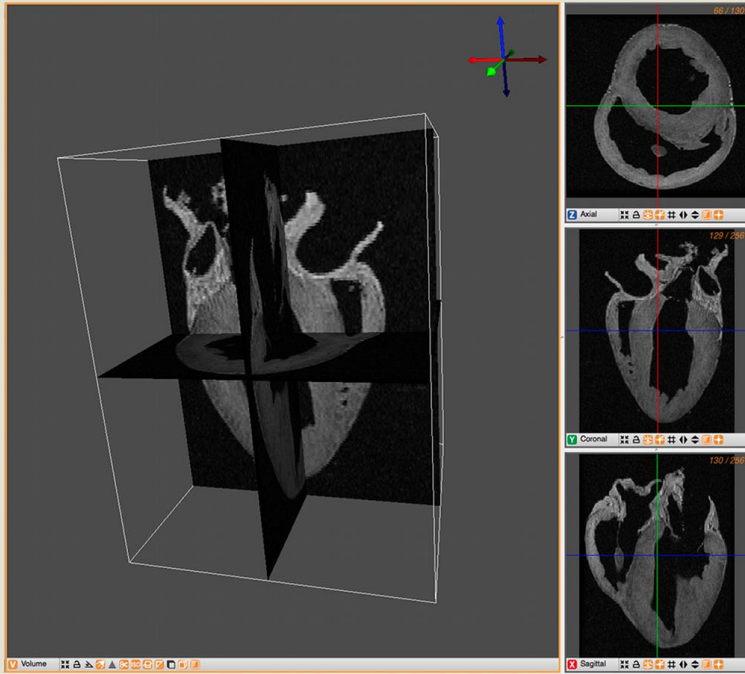
$$T^{\text{active}} = \sigma_a \mathbf{f} \mathbf{f}^T \quad \frac{d\mathbf{w}}{dt} = \mathbf{q}(\mathbf{w}; t_a, \lambda)$$

$$\sigma_a \equiv \sigma_a(\mathbf{w}; t_a, \lambda)$$

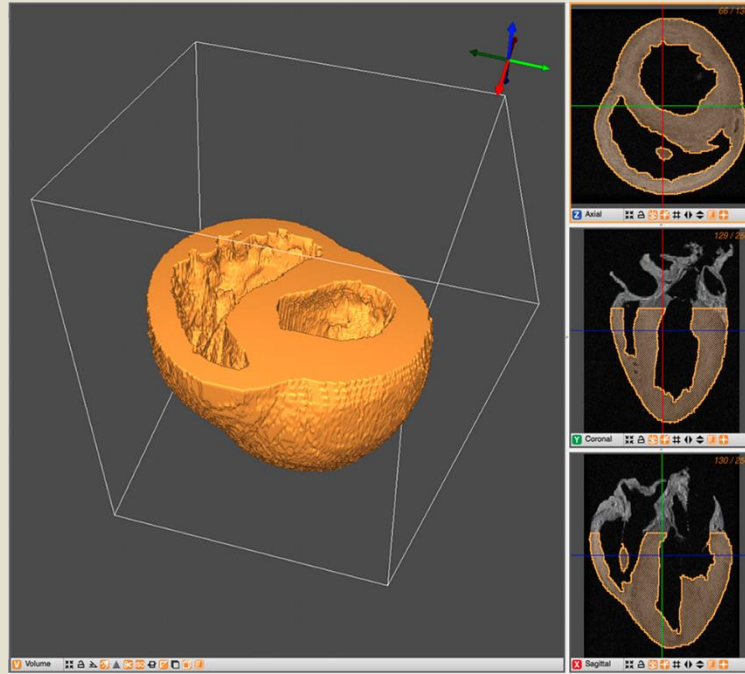
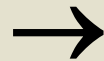
$$\begin{cases} \frac{d\bar{\mathbf{w}}}{dt} = \bar{\mathbf{q}}(\bar{\mathbf{w}}, t_a, \mathbf{U}) \\ K(\bar{\mathbf{w}}, \mathbf{U}, \mathbf{P}) = 0 \end{cases}$$

$$\mathcal{J}(\mathbf{U}_{k+1}^j, \mathbf{P}_{k+1}^j) \begin{bmatrix} \Delta \mathbf{U} \\ \Delta \mathbf{P} \end{bmatrix} = \begin{bmatrix} -\mathbf{r}_u(\mathbf{U}_{k+1}^j, \mathbf{P}_{k+1}^j) \\ -\mathbf{r}_p(\mathbf{U}_{k+1}^j, \mathbf{P}_{k+1}^j) \end{bmatrix}$$

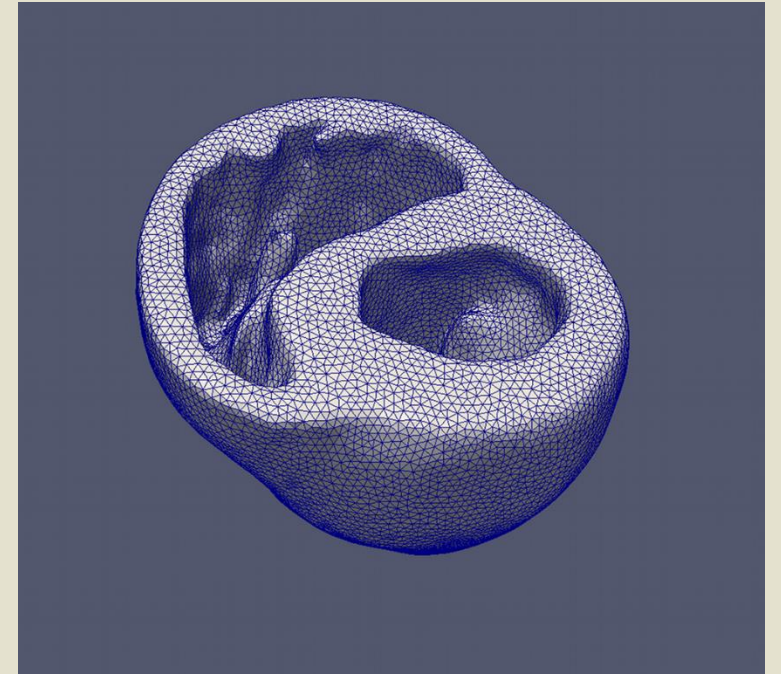
TOOLCHAIN



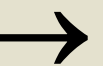
RAW DATA



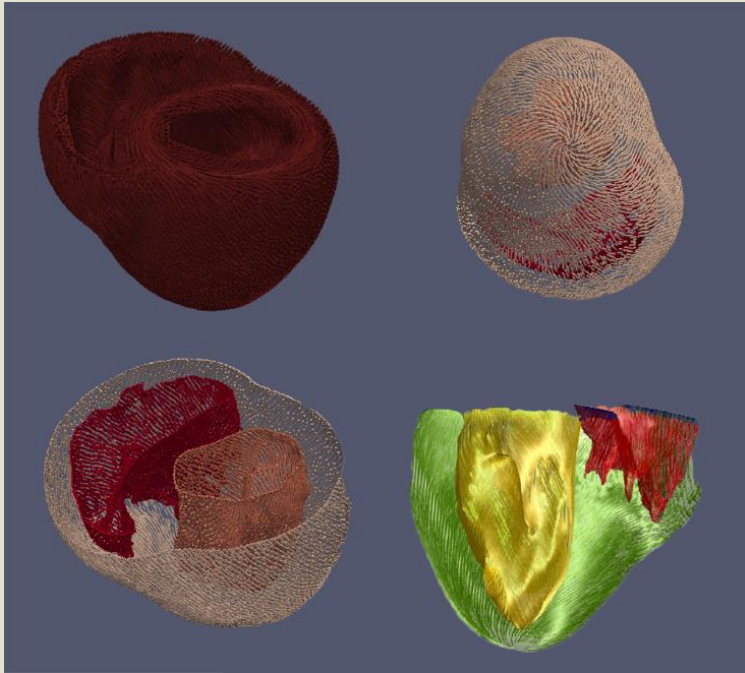
SEGMENTATION



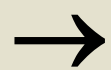
VOLUME MESH



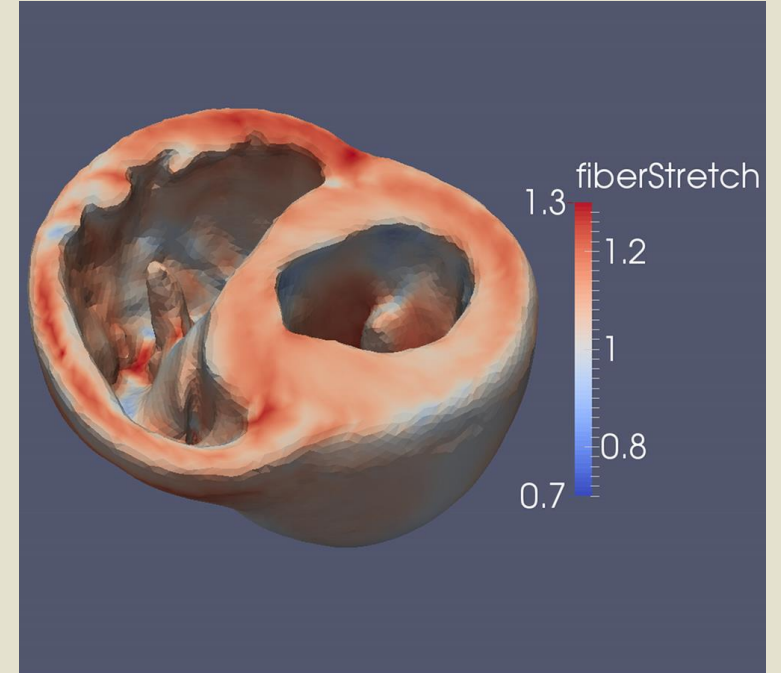
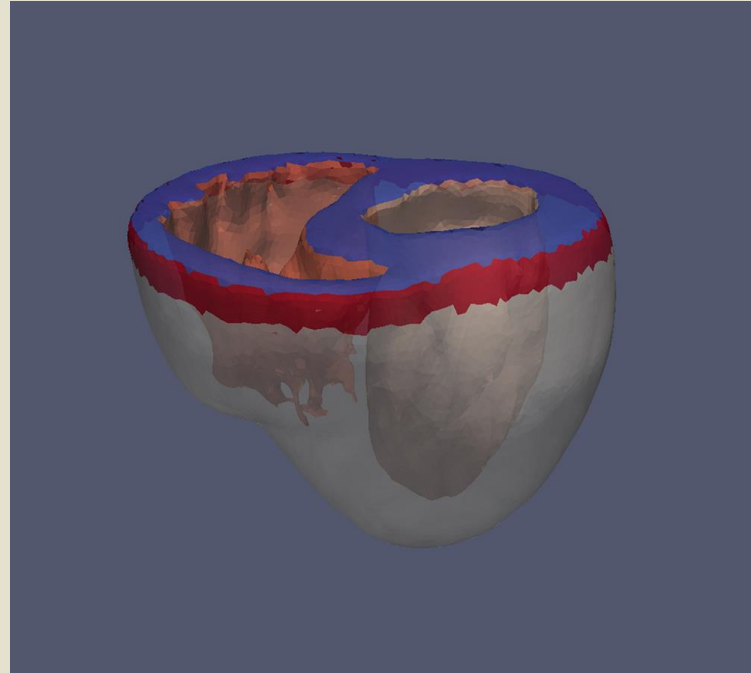
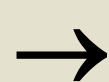
TOOLCHAIN



FIBER GENERATION

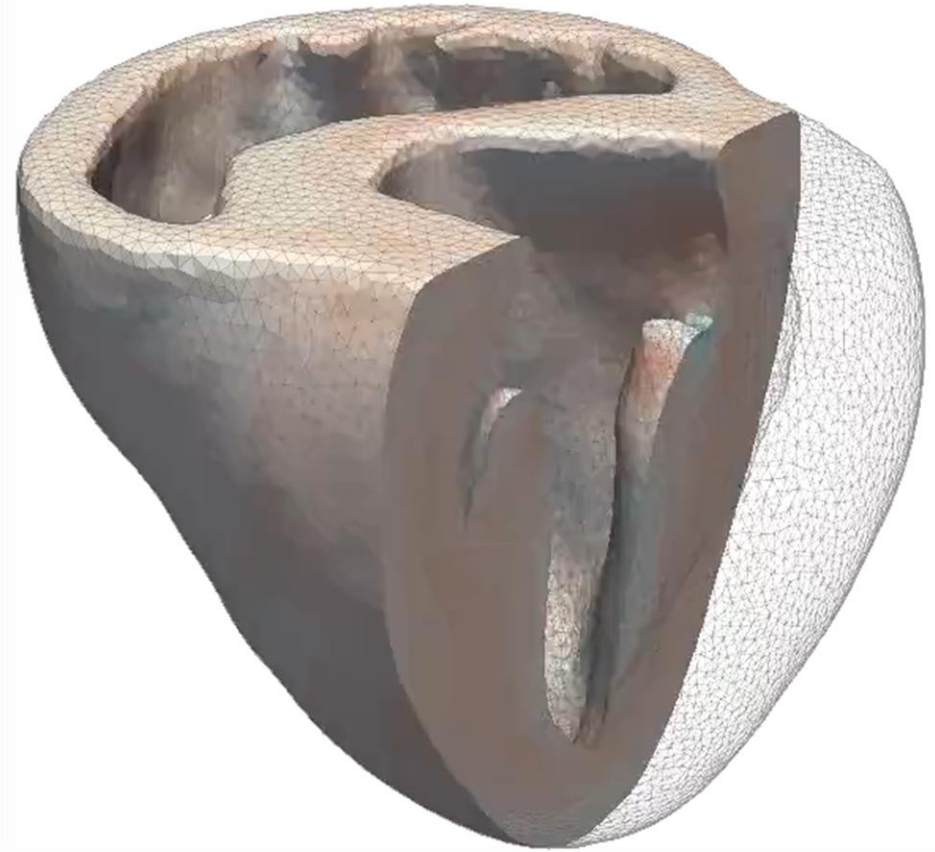
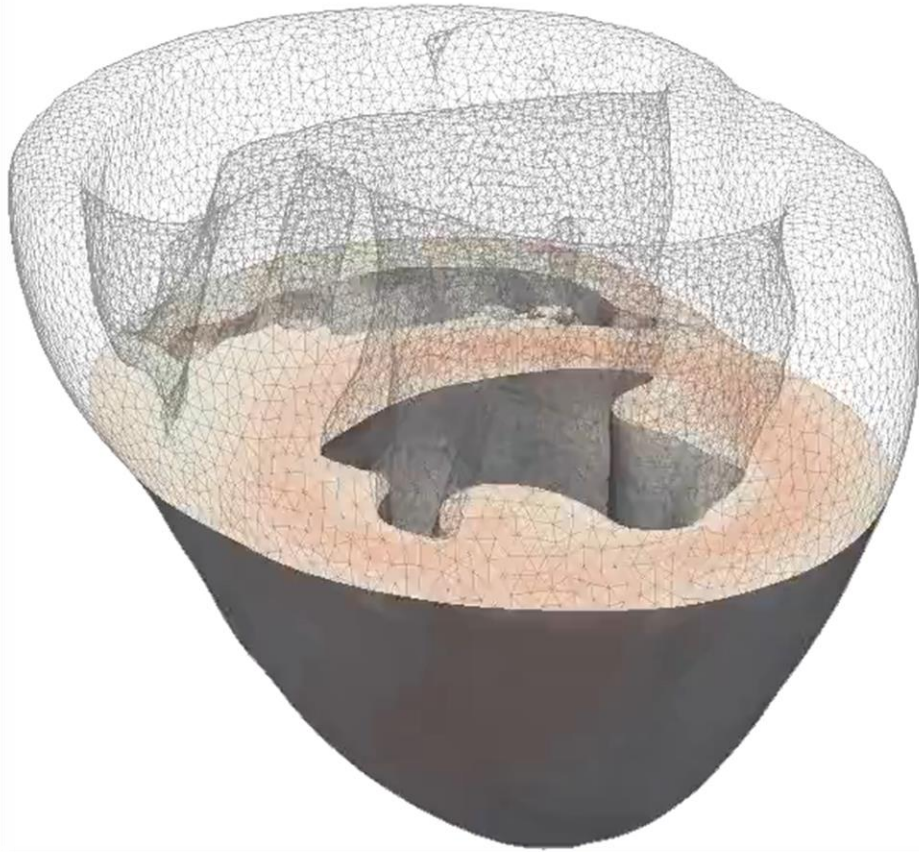


BOUNDARY CONDITIONS

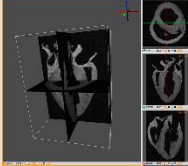


ANALYSIS

RESULTS



THE PIPELINE



MEDICAL IMAGING

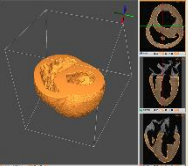
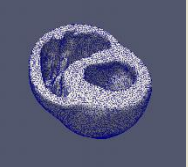
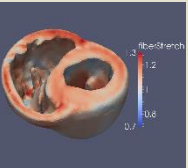


IMAGE SEGMENTATION



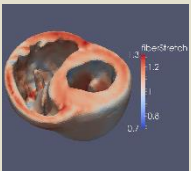
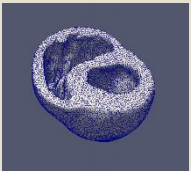
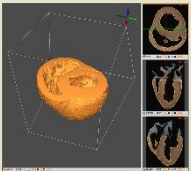
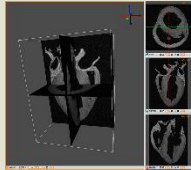
MESH GENERATION



ANALYSIS

CLINICAL APPLICATION

THE PIPELINE



MEDICAL IMAGING



IMAGE SEGMENTATION



MESH GENERATION



ANALYSIS



CLINICAL APPLICATION

THE PIPELINE

MEDICAL IMAGING



IMAGE SEGMENTATION



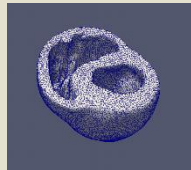
MESH GENERATION



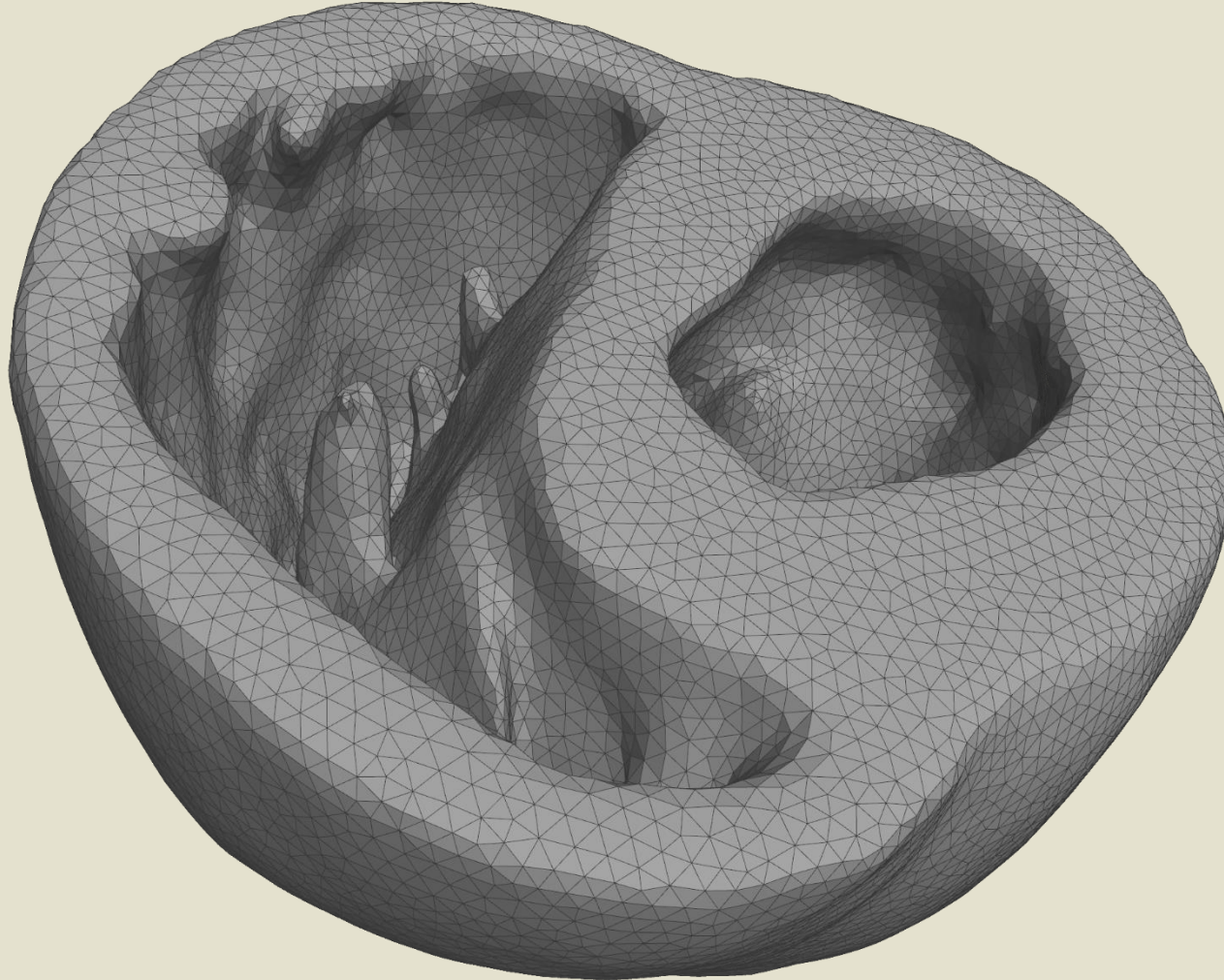
ANALYSIS



CLINICAL APPLICATION

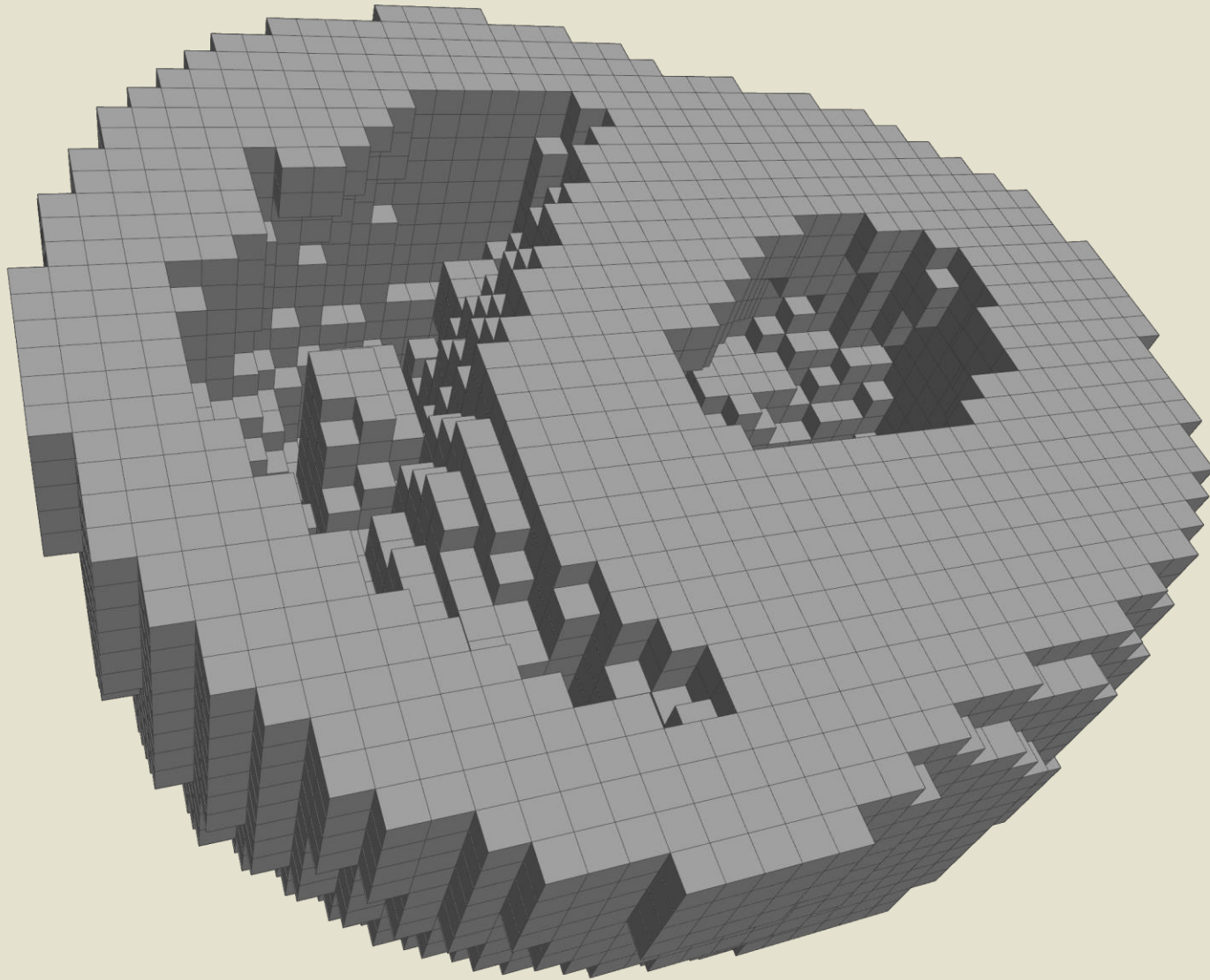


AUTOMATIC MESH GENERATION



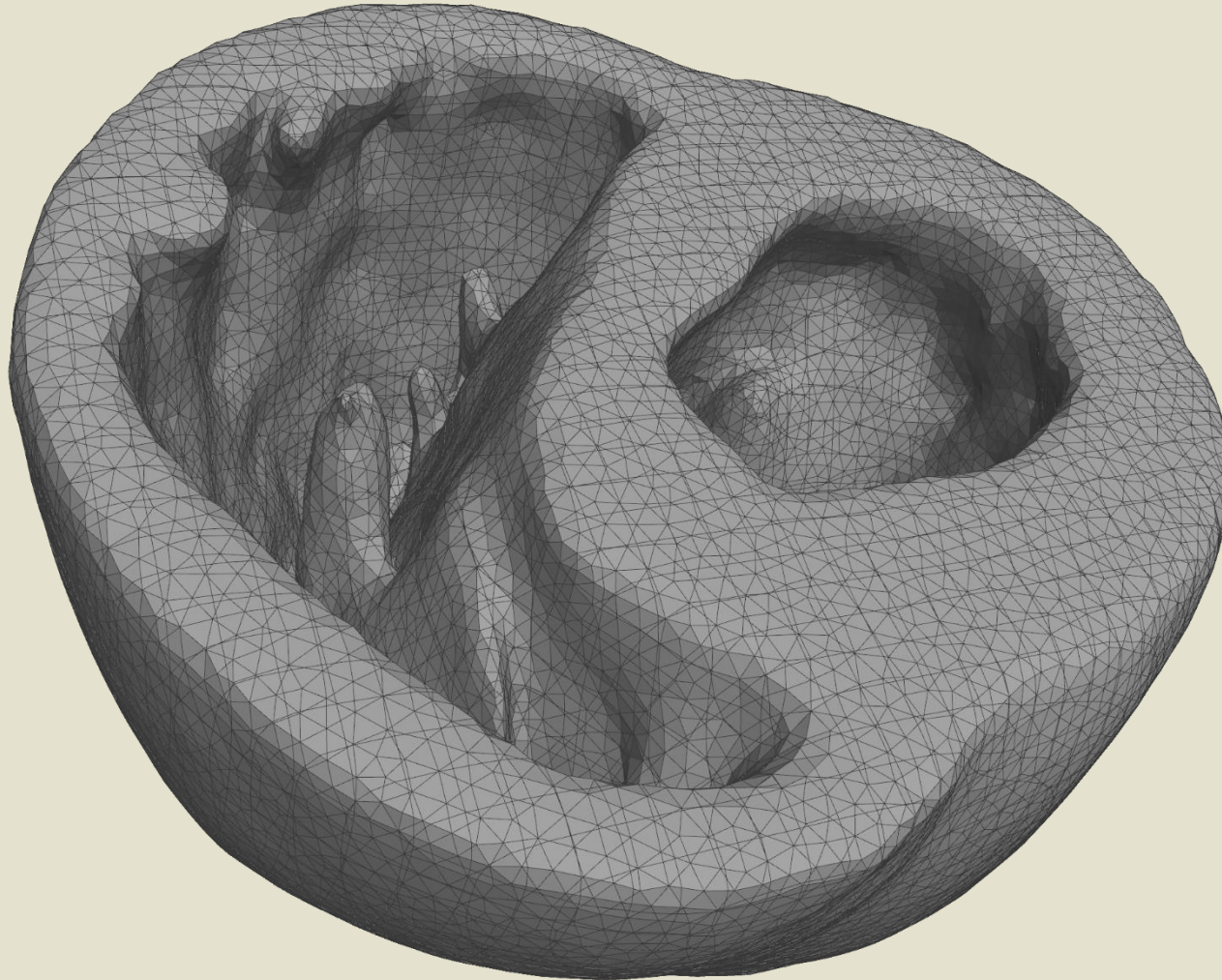
1. Given a boundary representation (b-rep) of the object

AUTOMATIC MESH GENERATION



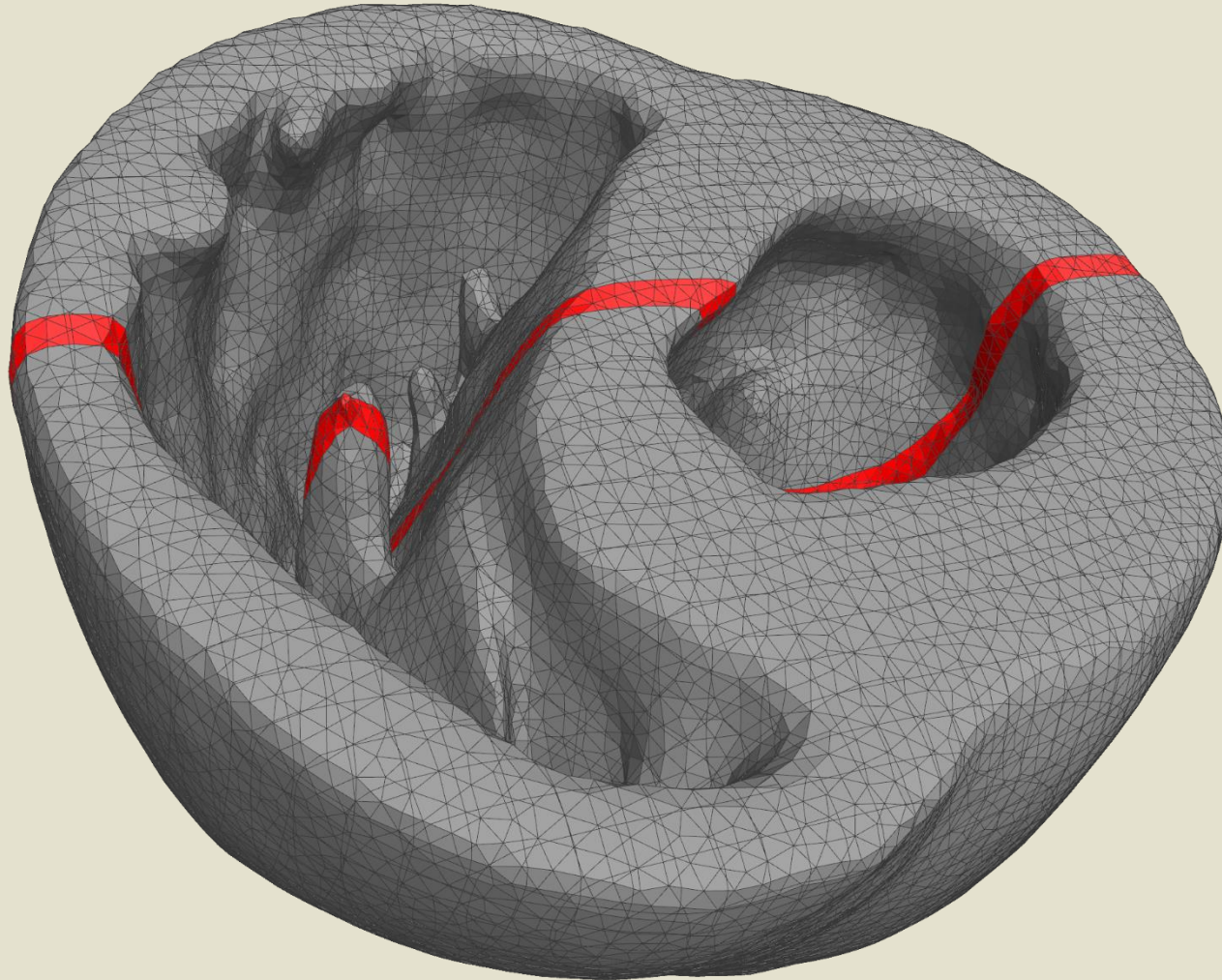
2. Create bounding hex mesh

AUTOMATIC MESH GENERATION



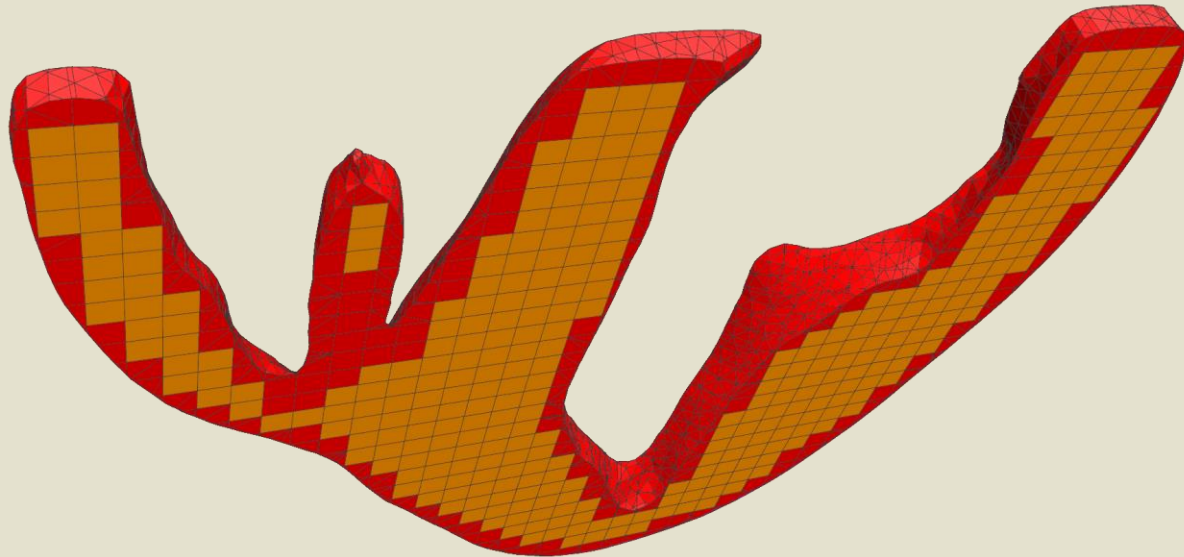
3. “Sculpt” the hex mesh with the b-rep

AUTOMATIC MESH GENERATION



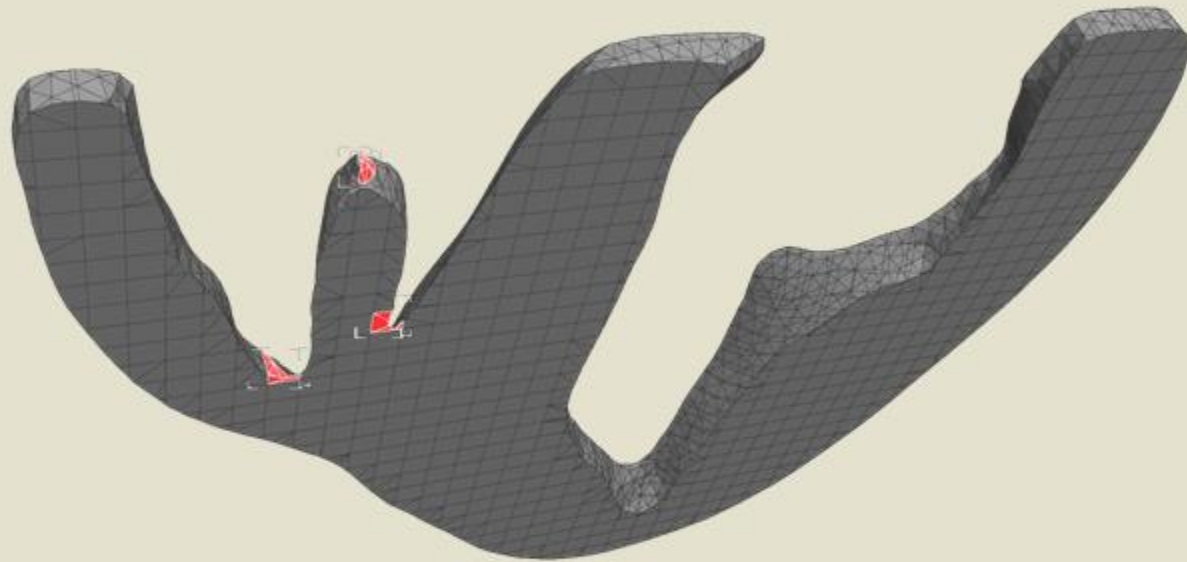
Arbitrary polyhedral
elements result

AUTOMATIC MESH GENERATION



Arbitrary polyhedral
elements result

AUTOMATIC MESH GENERATION



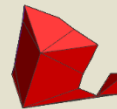
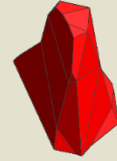
Arbitrary polyhedral
elements result

AUTOMATIC MESH GENERATION

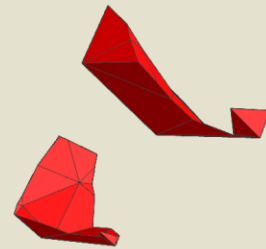
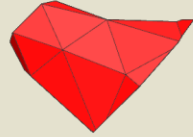


Arbitrary polyhedral
elements result

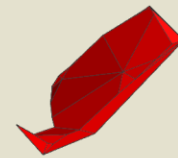
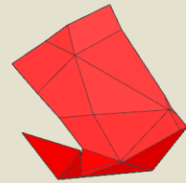
AUTOMATIC MESH GENERATION



AUTOMATIC MESH GENERATION



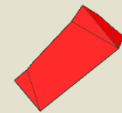
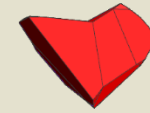
AUTOMATIC MESH GENERATION



AUTOMATIC MESH GENERATION



AUTOMATIC MESH GENERATION



COMPARISON

- Quadratic tetrahedra: 856k DOF
- Comparable polyhedral elements: 106k DOF
- Generally get order of magnitude reduction in system compared to tets!
- Heterogeneous conventional meshes can have their own (stability related) issues

THE PIPELINE

MEDICAL IMAGING



IMAGE SEGMENTATION



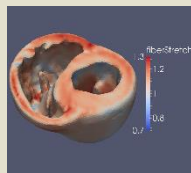
MESH GENERATION



ANALYSIS

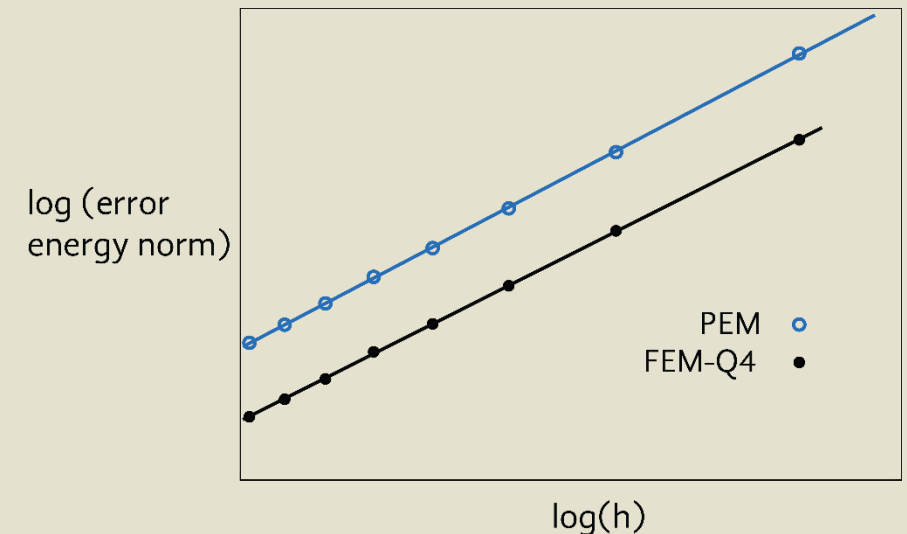
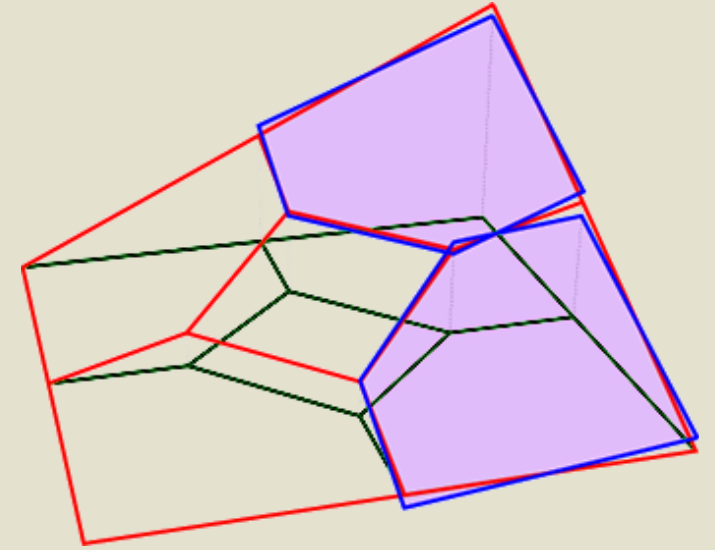


CLINICAL APPLICATION



THE PARTITIONED ELEMENT METHOD

- A new, FE-like method that accommodates essentially arbitrary polyhedral elements
- Allows for fast, robust meshing – no longer a bottleneck
- Shape functions are discrete discontinuous, piecewise linear functions over partitions of physical element
- Converges at the same rate as FEM
- PEM enjoys FEM-like BC enforcement and quadrature efficiency, without the strict topological restrictions on elements



THE PIPELINE

MEDICAL IMAGING



IMAGE SEGMENTATION



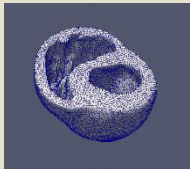
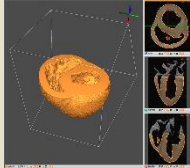
MESH GENERATION



ANALYSIS



CLINICAL APPLICATION



THE PIPELINE

MEDICAL IMAGING



IMAGE SEGMENTATION



B-REP GENERATION



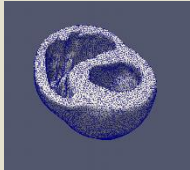
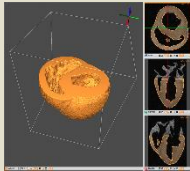
MESH GENERATION



ANALYSIS



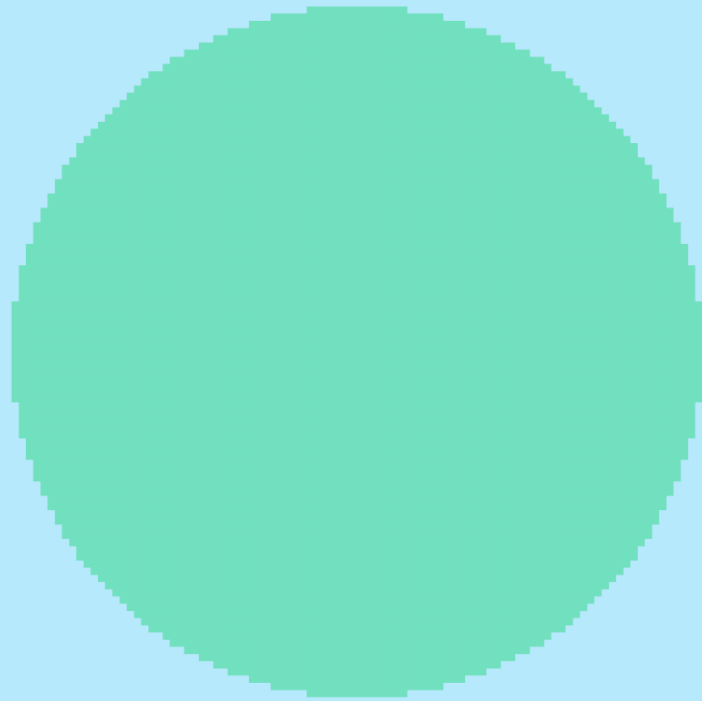
CLINICAL APPLICATION



OBJECTIVES

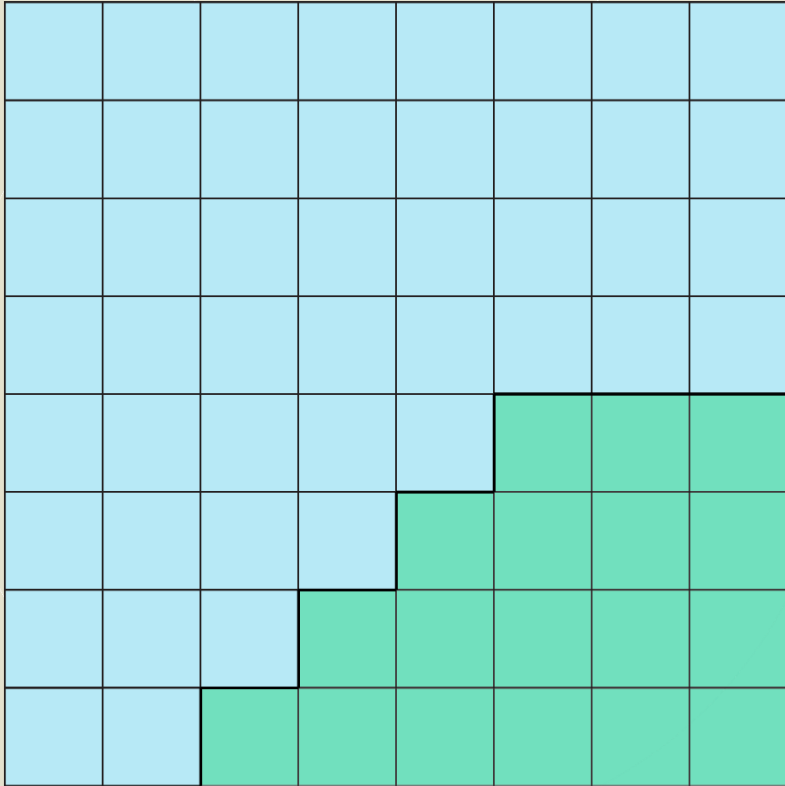
- Given 3D point intensity values, seek to
 - identify the different materials in a scan (**segmentation**) and
 - define their facetized boundaries (**b-rep generation**)
- Seek to:
 1. Minimize user interaction
 2. Produce an explicit definition of a facetized, watertight boundary representation
 3. Robust and reproducible
- For now, assume segmentation as input (manual, level sets, etc.)

VORONOI-BASED B-REP GENERATION



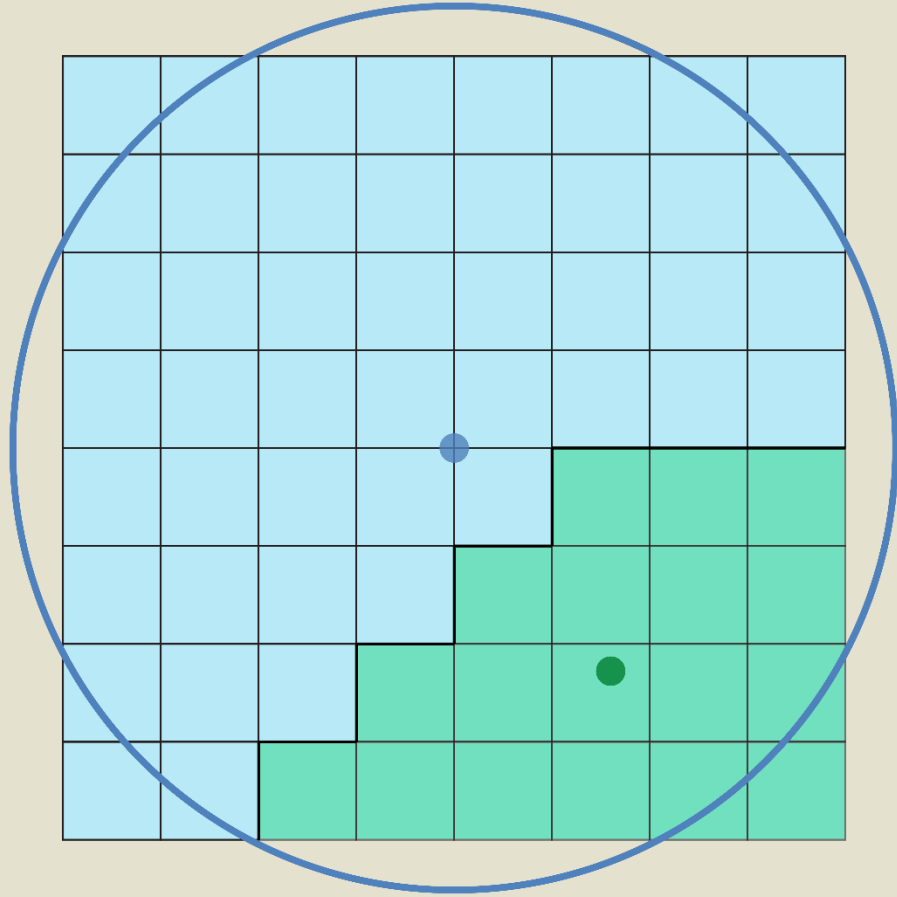
Use segmented
image as input –
each voxel
assigned a region

VORONOI-BASED B-REP GENERATION



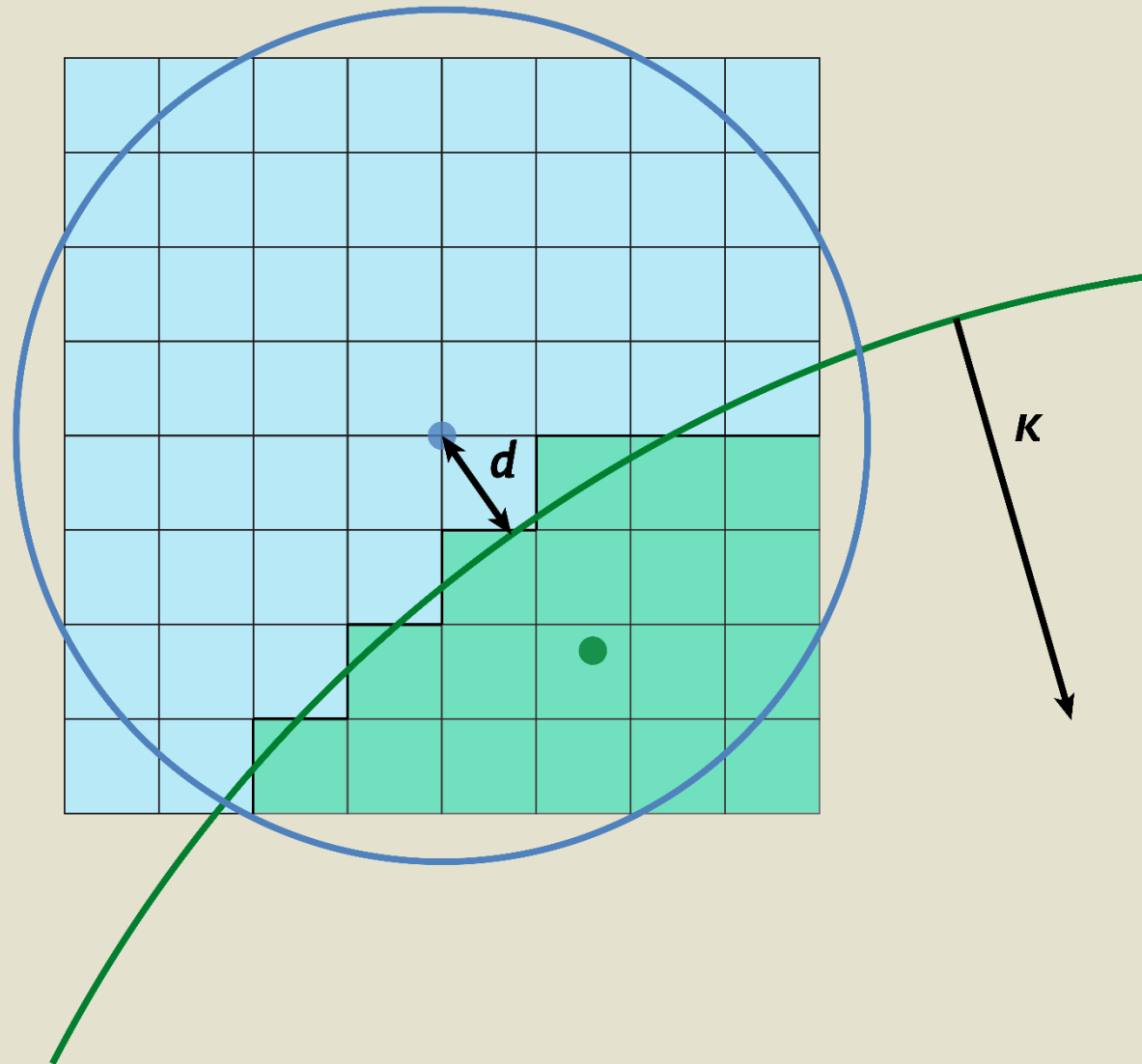
Consider a
window in the
segmented image

VORONOI-BASED B-REP GENERATION



Identify a disc that shares the same area and centroid of the entire window

VORONOI-BASED B-REP GENERATION

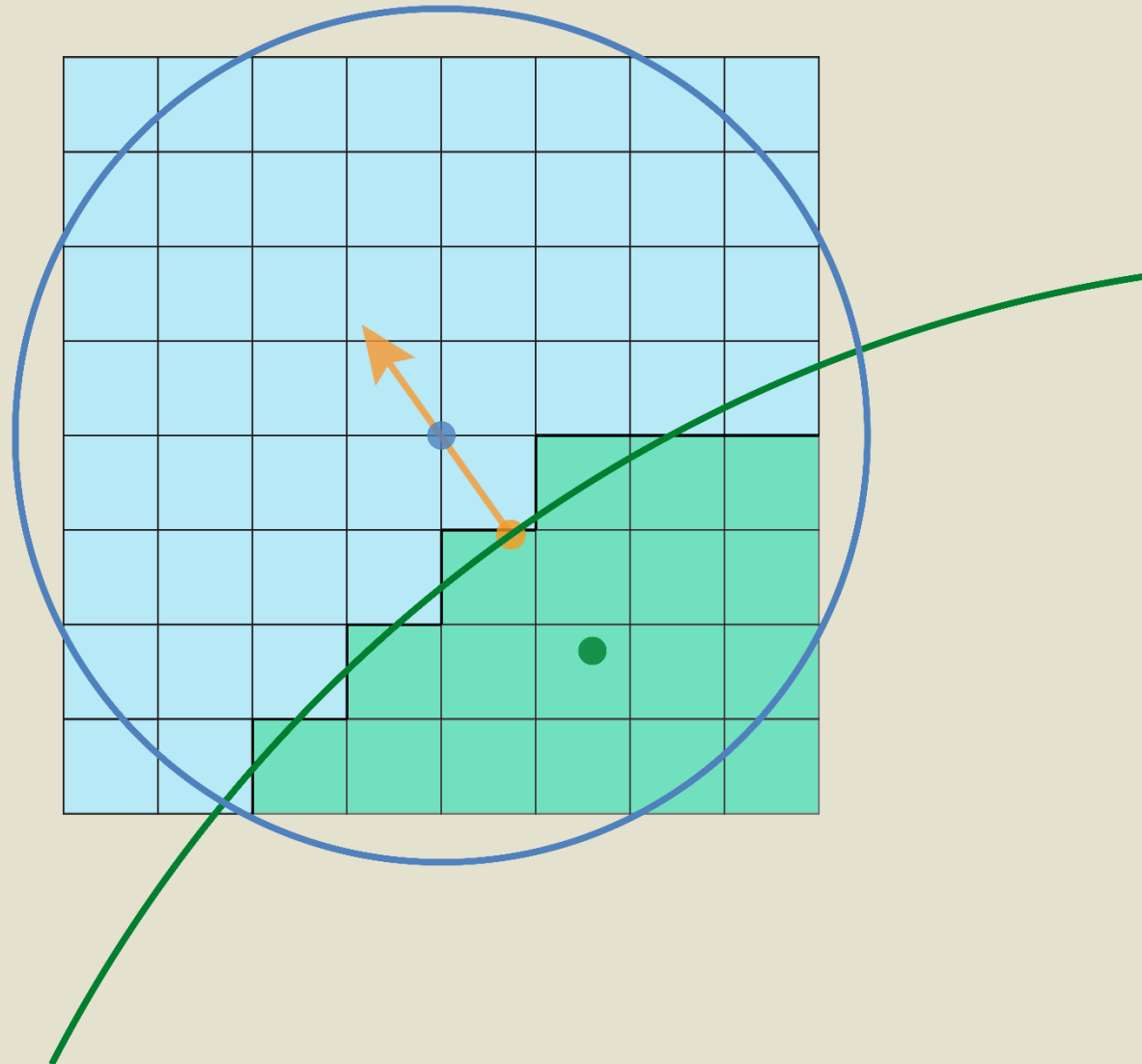


Approximate interface
with circular arc

Match the area and
centroid of material with
the area and centroid of
the intersecting disc.

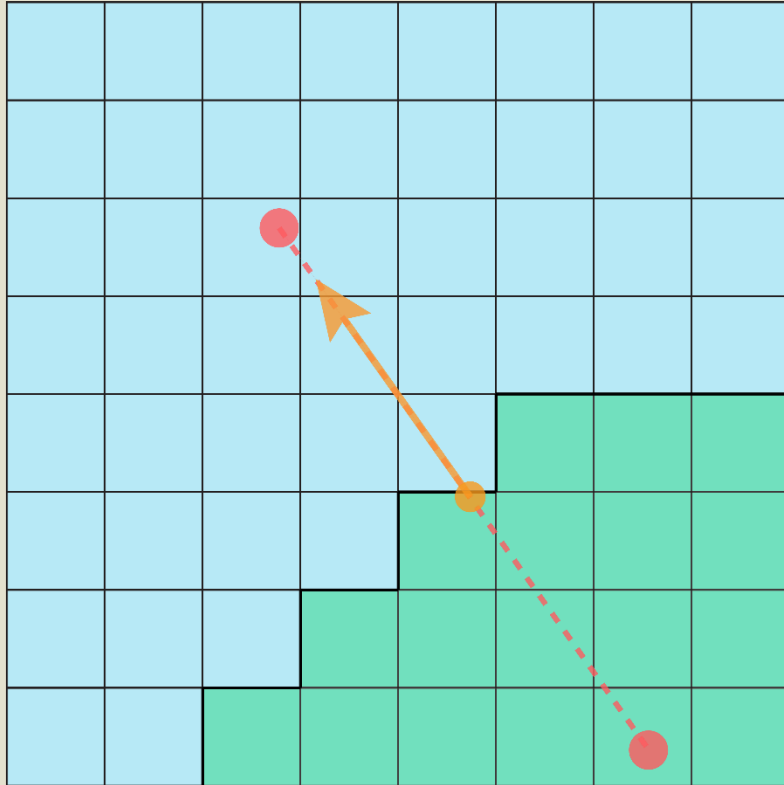
Results in nonlinear system
of equations in d and K .

VORONOI-BASED B-REP GENERATION



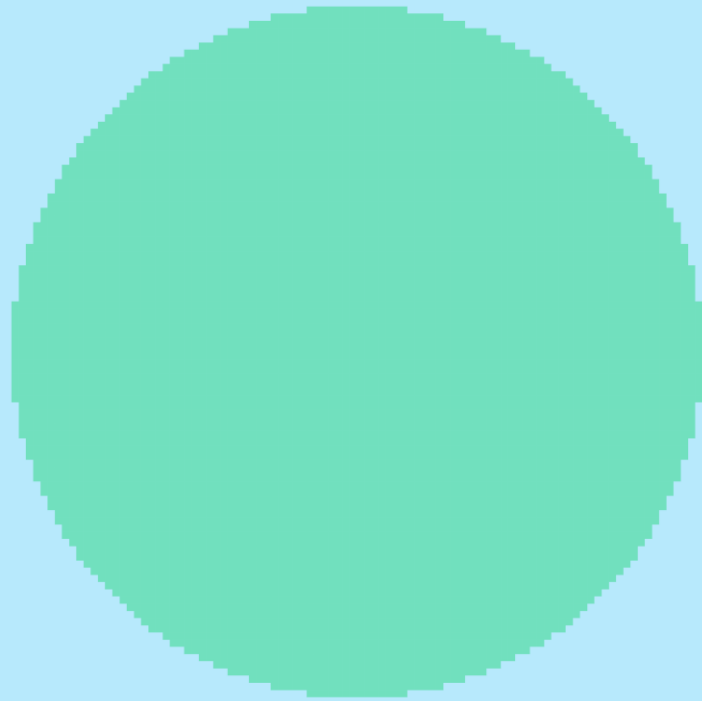
Identify the discrete point-direction pair defined by these geometric constructs

VORONOI-BASED B-REP GENERATION

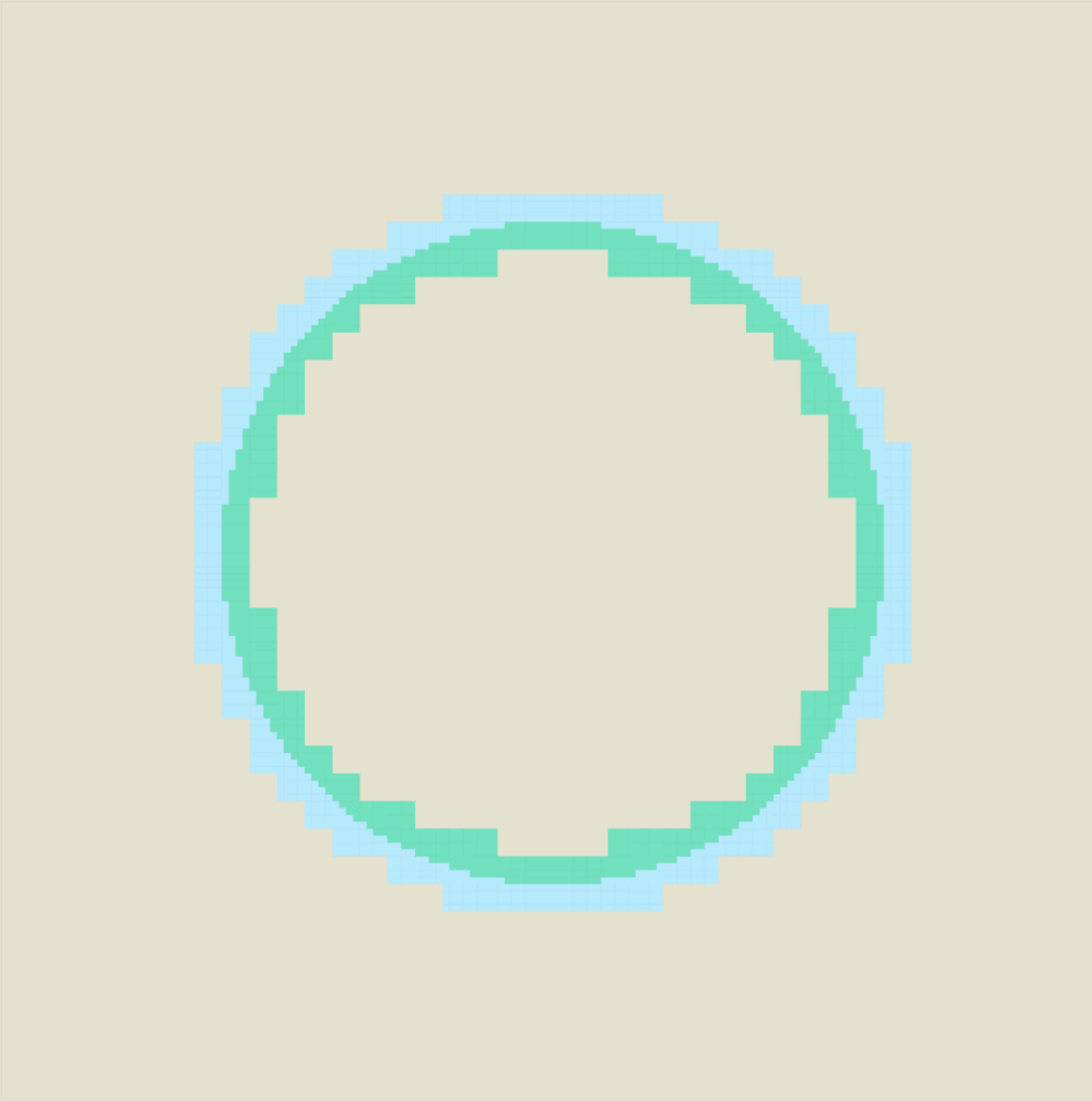


Introduce Voronoi
site pair based on
point-direction
pair

VORONOI-BASED B-REP GENERATION

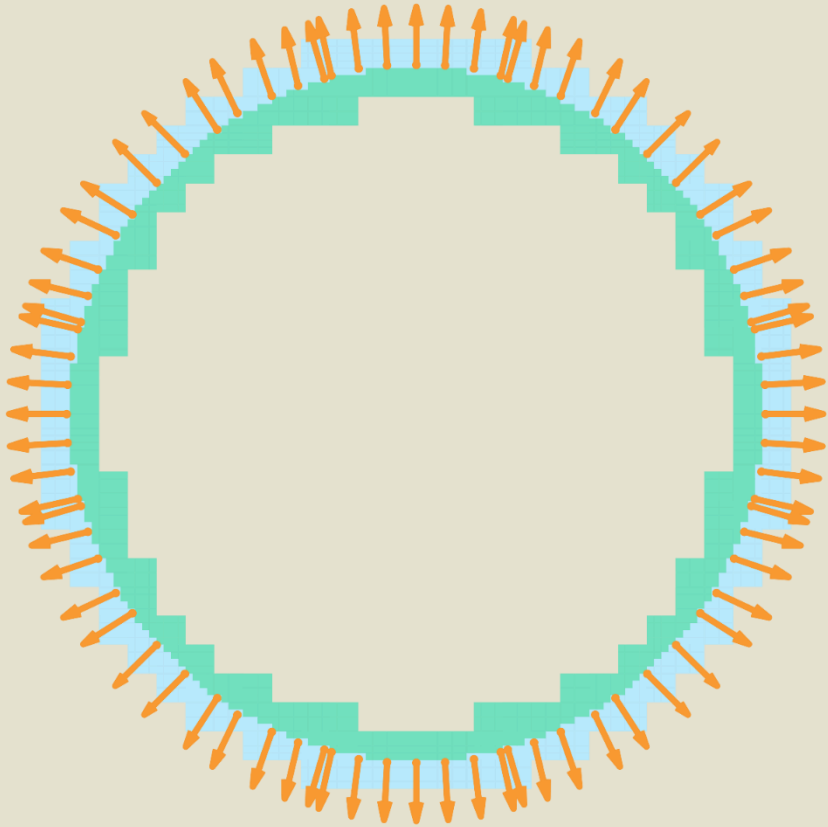


VORONOI-BASED B-REP GENERATION



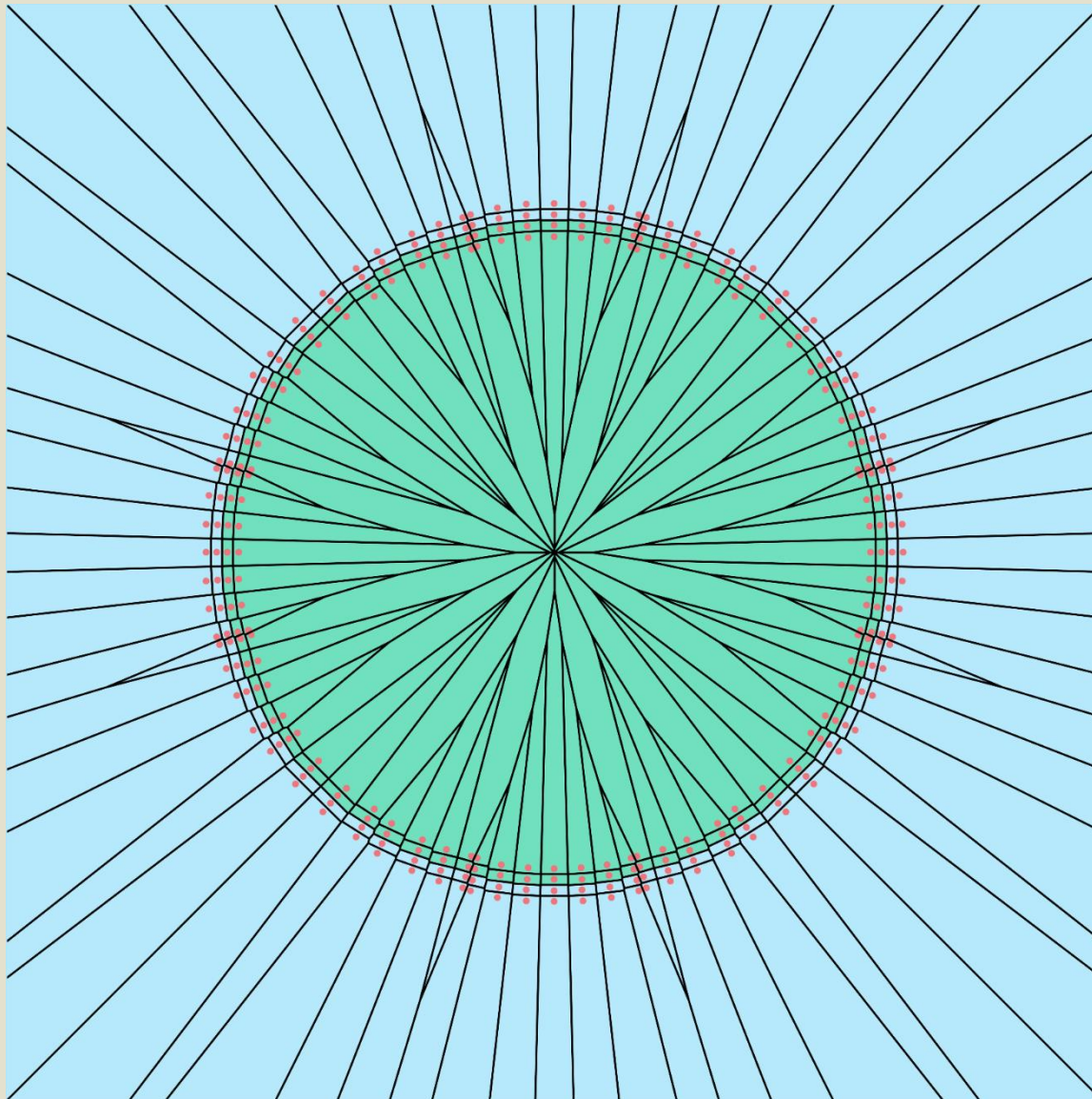
Identify windows
that have multiple
materials

VORONOI-BASED B-REP GENERATION



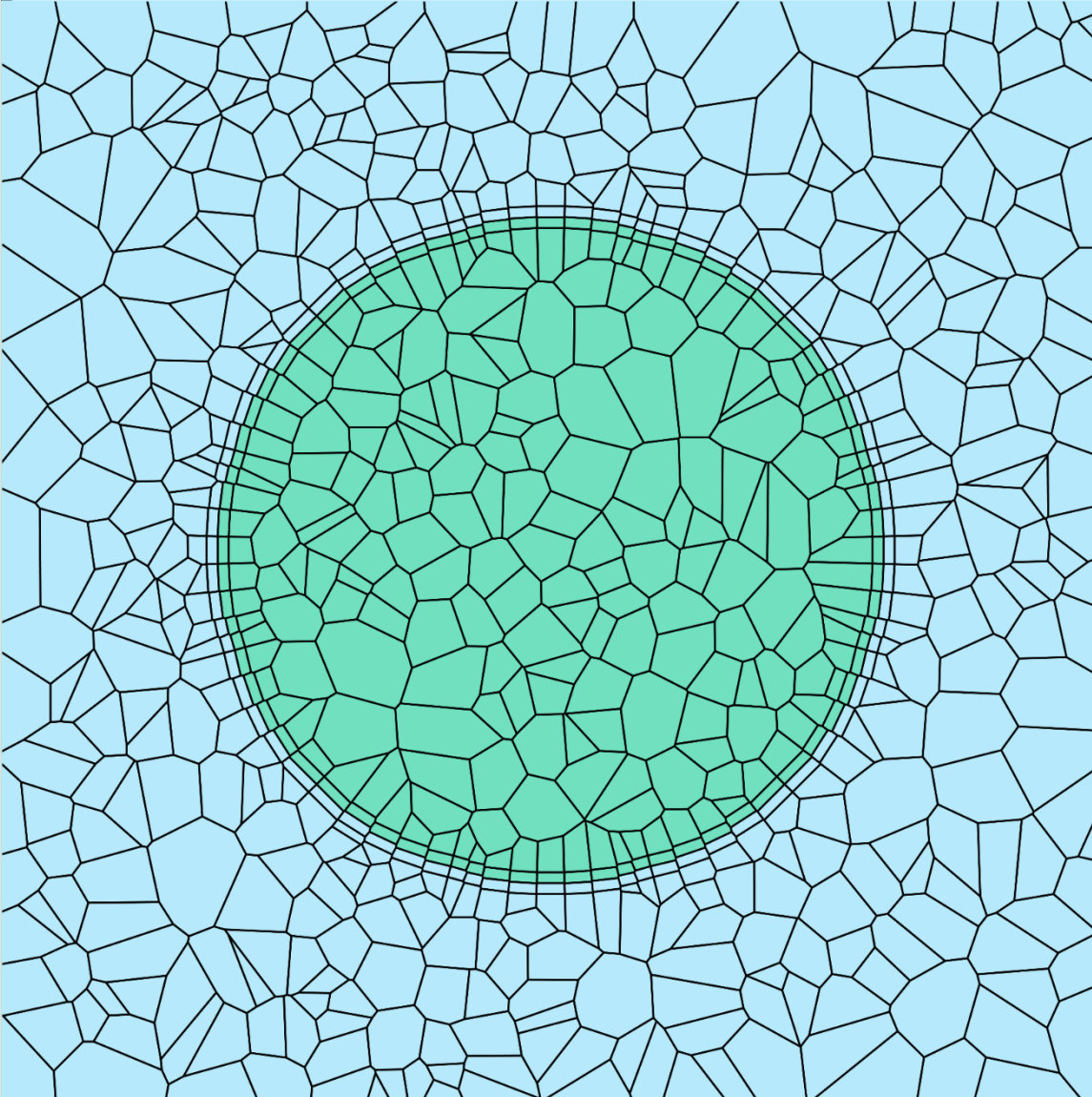
Compute discrete
point-direction
pair for each
window

VORONOI-BASED B-REP GENERATION



Introduce site
pairs

VORONOI-BASED B-REP GENERATION



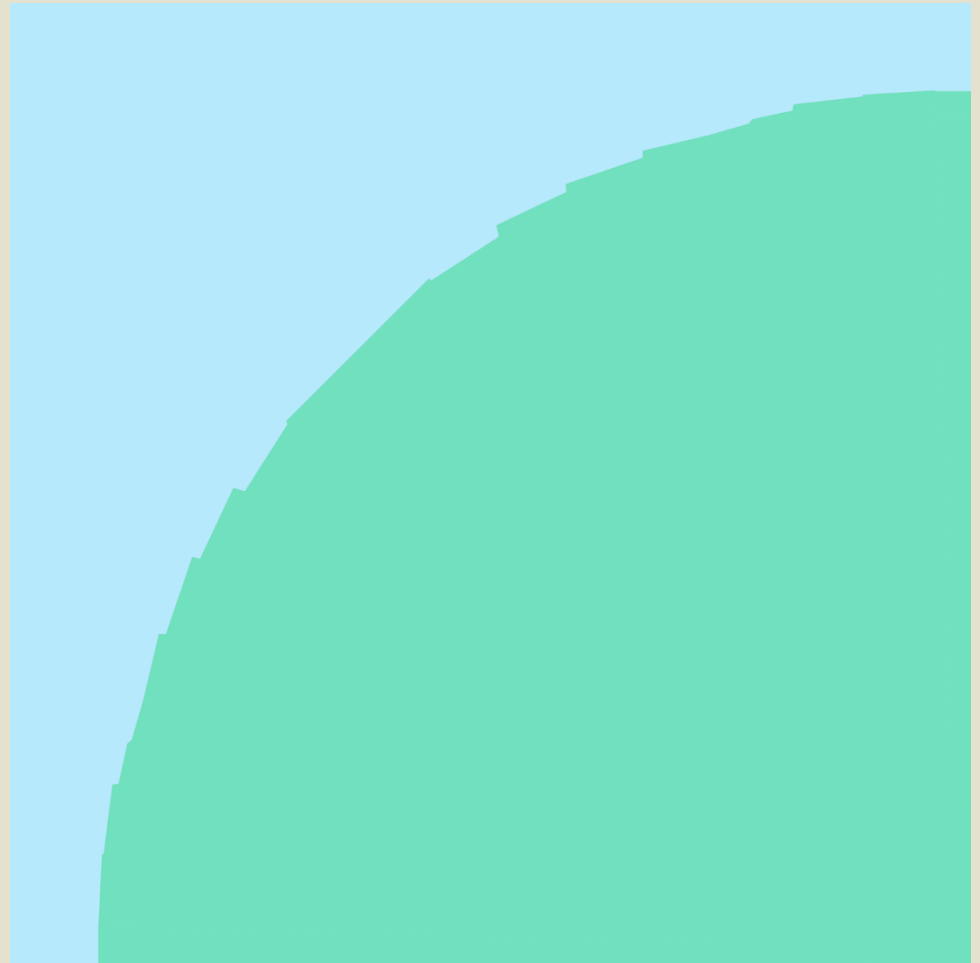
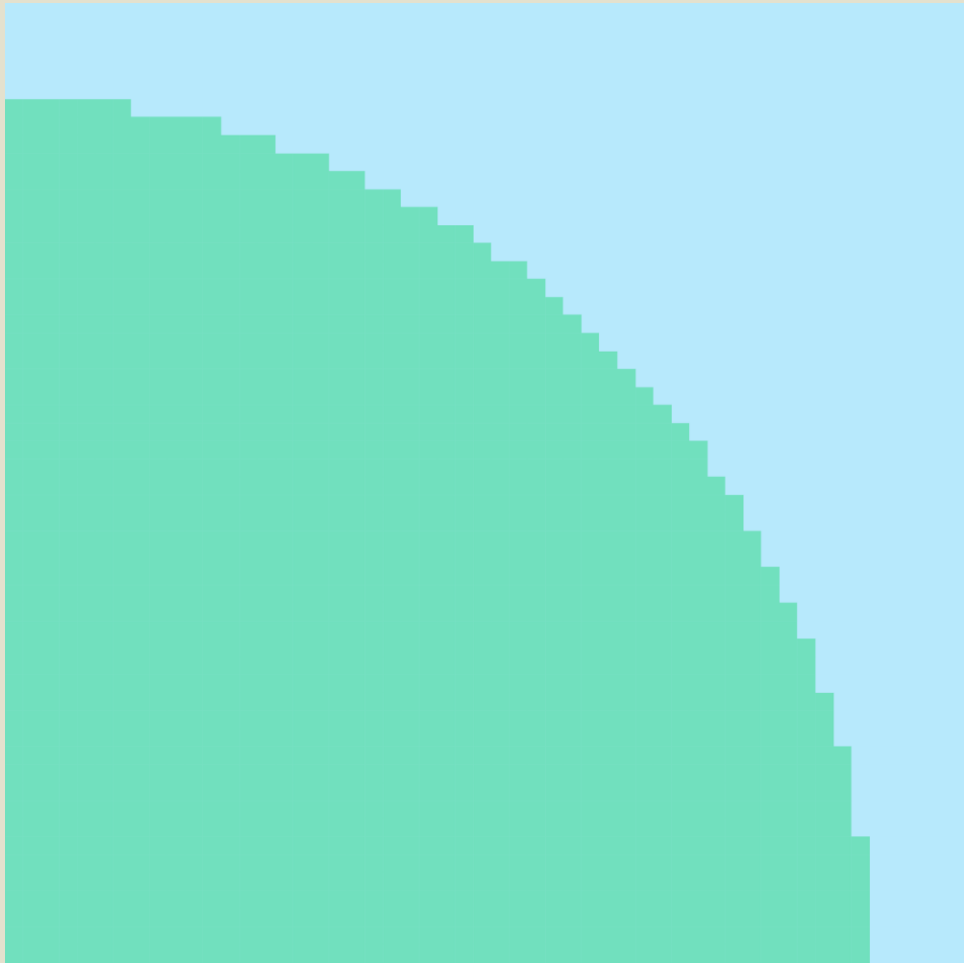
Introduce
additional sites
and perform
Voronoi partition

VORONOI-BASED B-REP GENERATION

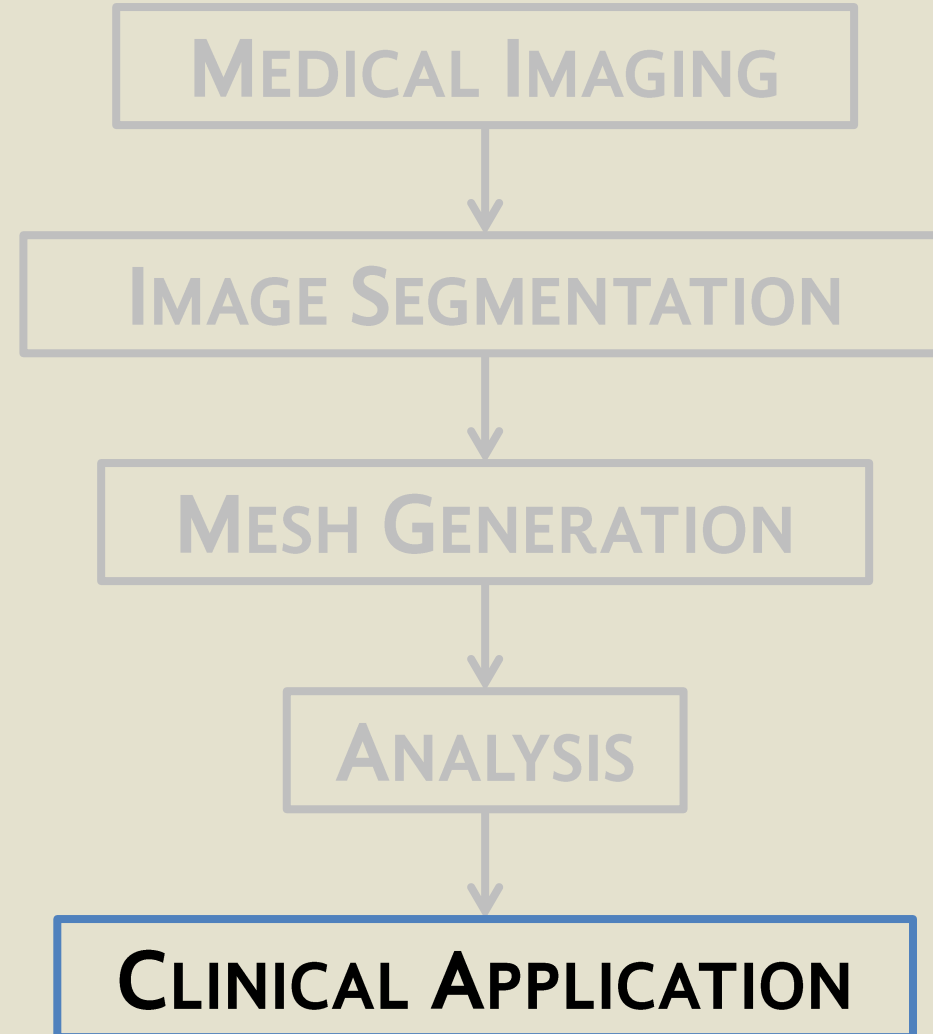


Resulting material
labeling from
Voronoi partition

VORONOI-BASED B-REP GENERATION

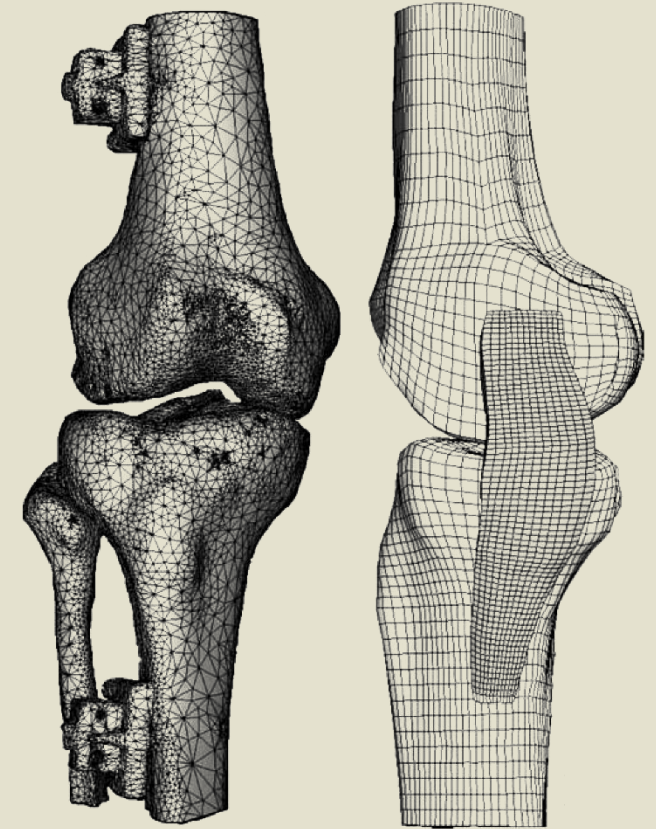


THE PIPELINE



CLINICAL APPLICATION

- Potential for to play important analytic and predictive role in medical applications
 - Improved diagnosis and treatment
 - Identify causes of pathology
 - Surgical design/planning
 - Computer-assisted surgery (real-time)
 - Haptic technologies/surgeon training



Gardiner JC, Weiss JA. *Subject-specific finite element analysis of the human medial collateral ligament during valgus knee loading.* Journal of Orthopaedic Research, vol. 21, pp. 1098-1106, 2003

“CLINICAL COMPUTATION”

- An automated, patient-specific process provides the means to run lots of simulations quickly, and get lots of data
- Clinical trials via simulation
- Additional considerations needed:
 - Material properties
 - Boundary conditions
 - UQ, V&V
 - HPC

One day:

“With a 95% confidence level, changing the drilling angle by 3% for an ACL graft reduces the average patellofemoral stress 10-15%”

THANK YOU

**UNIVERSITY OF
CALIFORNIA, DAVIS**

MARK RASHID

CELERIS LLC

ANDREW BALDWIN

ALIPASHA SADRI

**LAWRENCE LIVERMORE
NATIONAL LABORATORY**

FRED STREITZ

DAVID RICHARDS

JEAN-LUC FATTEBERT

**INTERNATIONAL BUSINESS
MACHINES**

VIATCHESLAV GUREV

JEREMY RICE

KRELL INSTITUTE

TOO MANY TO LIST!

This project incorporates tools whose development was funded in part by the NIH through the NHLBI grant: The Cardiovascular Research Grid (R24HL085343)

Financial support from DOE CSGF grant DE-FG02-97ER25308 is gratefully acknowledged

The work of LLNL authors was performed under the auspices of the U.S. Department of Energy by Lawrence Livermore National Laboratory under Contract DE-AC52-07NA27344. Lawrence Livermore National Security, LLC. LLNL-PRES-675401